Helmholtz-Zentrum Dresden-Rossendorf (HZDR)

Comparable radiation response of ex vivo and in vivo irradiated tumor samples determined by residual γH2AX

Rassamegevanon, T.; Löck, S.; Baumann, M.; Krause, M.; von Neubeck, C.;

Comparable radiation response of *ex vivo* and *in vivo* irradiated tumor samples determined by residual γH2AX

Treewut Rassamegevanon[1], Steffen Löck[1,2,3], Michael Baumann[1,2,3,4,5,6], Mechthild Krause[1,2,3,4,5], Cläre von Neubeck[1,3]

1   OncoRay – National Center for Radiation Research in Oncology, Faculty of Medicine and University Hospital Carl Gustav Carus, Technische Universität Dresden, Helmholtz-Zentrum Dresden - Rossendorf, Dresden, Germany;

2   Department of Radiotherapy and Radiation Oncology, Faculty of Medicine and University Hospital Carl Gustav Carus, Technische Universität Dresden, Dresden, Germany

3   German Cancer Consortium (DKTK), Partner Site Dresden, and German Cancer Research Center (DKFZ), Heidelberg, Germany

4   Helmholtz-Zentrum Dresden - Rossendorf, Institute of Radiooncology – OncoRay, Dresden, Germany

5   National Center for Tumor Diseases (NCT), Partner Site Dresden, Germany: German Cancer Research Center (DKFZ), Heidelberg, Germany; Faculty of Medicine and University Hospital Carl Gustav Carus, Technische Universität Dresden, Dresden, Germany, and; Helmholtz Association / Helmholtz-Zentrum Dresden - Rossendorf (HZDR), Dresden, Germany

6   German Cancer Research Center (DKFZ), Heidelberg, Germany

Running title: Radiation response *in vivo* vs. *ex vivo*

Keywords: γH2AX foci, intrinsic radiation sensitivity, predictive biomarker, radiation therapy

Figure: 3

Table: 1

Supplementary figure: 4

Supplementary table: 2

Corresponding author: Treewut Rassamegevanon, OncoRay - National Center for Radiation Research in Oncology, Faculty of Medicine and University Hospital Carl Gustav Carus, Technische Universität Dresden, Fetscherstrasse 74, 01307 Dresden,

Declarations:

Ethics approval and consent to participate:

The local committee on ethics of animal experimentation approved all experiments.

Availability of data and material:

The dataset generated during the current study is available from the corresponding author on reasonable request.

Financial support:

This work was supported by a grant of the Federal Ministry of Education and Research (BMBF 02NUK035C)

Author's contribution:

TR and CvN performed the experiments and wrote the manuscript. TR analyzed the data and performed the statistical analysis. CvN designed the animal study. SL validated the statistical analysis. CvN, MK and MB had the project idea, wrote the concept for grant application, supervised the study and contributed to data interpretation. All authors read and approved the final manuscript.

Abstract

Purpose: a) To investigate if an *ex vivo* cultured and irradiated tumor biopsy reflects and predicts the radiation response of the corresponding *in vivo* irradiated tumor measured with the DNA double strand break marker γH2AX foci.

Materials and methods: Five human head and neck squamous cell carcinoma (hHNSCC) xenograft models were used. Fine needle biopsies were taken from anesthetized tumor-bearing NMRI nude mice prior to *in vivo* single dose irradiation (0, 2, 4, or 8 Gy) under ambient blood flow. Biopsies were *ex vivo* reoxygenated and irradiated with equivalent doses. Tumors and biopsies were fixed 24 h post irradiation, and γH2AX foci were assessed in oxygenated tumor regions.

Results: Linear regression analysis showed comparable slopes of the residual γH2AX foci dose response curves in four out of five hHNSCC models when *in vivo* and *ex vivo* cohorts were compared. The slopes from *ex vivo* biopsies and *in vivo* tumors could classify the respective tumor model as sensitive or resistant according to the intrinsic radiation sensitivity (TCD_{50}).

Conclusion: The ability of *ex vivo* irradiated tumor biopsies to reflect and predict the intrinsic radiation response of *in vivo* tumors increases the translational potential of the *ex vivo* γH2AX foci assay as a diagnostic tool in clinical practice.

Introduction

The standard of care for advanced HNSCC comprises surgery followed by radio(chemo)therapy or, alternatively, primary radio(chemo)therapy with a total radiation dose of ~70 Gy for combined fractionation. Although a routine pathological investigation classifies tumor grade and stage prior to initiation of radio(chemo)therapy, the classification generally disregards the patient-dependent intrinsic radiosensitivity, which importantly influences treatment outcome [1–4]. Thus, a predictive assay that supports physicians to prescribe an individualized radiation dose could improve treatment outcome and reduce excess toxicity [1–7].

One of the available molecular biomarkers for the determination of intrinsic radiosensitivity is the phosphorylated histone H2AX (γH2AX). Phosphorylation occurs within seconds after irradiation at serine 139 in vicinity of a DNA double strand break (DSB) [8]. The formed γH2AX foci are microscopically detectable and serve as a specific, sensitive, robust, and straightforward DNA DSB biomarker [9–14]. GammaH2AX foci demonstrated a promising capability in stratifying tumors according to their intrinsic radiosensitivity. Previously, residual γH2AX foci (24 h post irradiation) predicted the radiation response of *in vivo* irradiated

hHNSCC xenograft tumors [15,16]. Based on this, a clinical relevant *ex vivo* γH2AX foci assay was established, showing its predictive potential in specimens of established tumor models and surgical patient-derived biopsies by grouping them according to the known clinical radiosensitivity [17–20]. However, evidence that an *ex vivo* cultured and irradiated tumor biopsy can reflect and predict the radiation response of the corresponding *in vivo* irradiated tumor is still missing. In this study, fine needle biopsies were taken from xenotransplanted hHNSCC prior to a single dose irradiation to the tumor. The biopsies were exposed to radiation with equivalent doses and γH2AX foci, as a marker of DNA double strand breaks, were assessed in both *in vivo* tumors and *ex vivo* biopsies. This experimental design allowed for a matching comparison of radiation response between the *in vivo* and *ex vivo* scenario. The experimental tumor models were categorized according to the slopes of the dose-response curves (SDRC) of residual γH2AX foci, a potential radiation sensitivity predictor [15,18,19], and their radiation sensitivity based on previously determined data [15,16,21] to assess the prediction capability of the *ex vivo* assay.

Materials and Methods

Animal and experimental tumor models

Five established hHNSCC lines i.e., SKX, FaDu, Cal33, UT-SCC-5, and UT-SCC-45 were investigated. Characteristics of these tumor models [15,22,23] as well as their xenotransplantation were previously described [15,21,24]. In brief, 7 - 14 weeks old male and female NMRI (nu/nu) mice from the pathogen-free animal breeding facilities (Experimental Center and OncoRay, Faculty of Medicine, Technische Universität Dresden, Germany) were whole body irradiated with 4 Gy 2 - 5 days prior to transplantation (X-rays, Maxishot 200 Y.TU/320-D03, Yxlon Int., Hamburg, Germany; 200 kV, 20 mA; 0.5 mm Cu filter; dose rate 1 Gy/min). Small pieces of a source tumor were subcutaneously transplanted on the hind-leg of anesthetized mice (Ketamine ([Ketamin 500 Curamed®, Curamed Pharma, Karlsruhe, Germany] 100 mg/kg) and Xylazine ([Rompun®, Bayer Healthcare, Leverkusen, Germany] 10 mg/kg)). Microsatellite, histology, and volume doubling times were assessed for validation of tumor lines. The animal facilities and the experiments were approved by the regulatory authorities and followed the institutional guidelines as well as the German animal welfare regulations.

In vivo and *ex vivo* experimental settings

Figure 1 summarizes the workflow of the *in vivo* and *ex vivo* procedures. Animals bearing tumors with a maximum diameter of ~10x10 mm (~1 cm^2) were anesthetized and randomly allocated to the treatment arms. Fine needle biopsies (BioPince 18G, 1.3 mm, Angiotech-Medical Device Technologies Inc., Gainesville, USA) were taken. Tumor biopsies were

immediately transferred into petri dishes coated with 1.5% agarose (A9539, Sigma–Aldrich, Taufkirchen, Germany)). Biopsies were maintained in 2.5 ml Dulbecco's MEM culture medium supplemented with 2% HEPES, 1% Na pyruvate, 1% non-essential amino acids, 1% penicillin streptomycin (all Biochrom, Berlin, Germany); and 10% FCS (Sigma-Aldrich, Taufkirchen, Germany) at 37°C and 5% CO_2.

In vivo irradiation: After recovery from anesthesia, animals were intraperitoneally injected with 0.1 mg/g body weight pimonidazole (hypoxia marker; Natural Pharmacia International, Belmont, MA, USA) and 3.75 mg bromodeoxyuridine (BrdU; proliferation marker; SERVA electrophoresis, Heidelberg, Germany) 1 h prior to irradiation. Tumor-bearing legs were locally irradiated with single doses of 0, 2, 4, or 8 Gy of X-rays under ambient blood flow. Animals were sacrificed 24 h post irradiation. Tumors and the overlying skin were excised; sebaceous glands served as positive controls for pimonidazole incorporation. Tumors were fixed in 4% formalin and embedded in paraffin.

Ex vivo irradiation: tumor biopsies were incubated for 20 h prior to media supplementation and 4 h incubation with 8.5 µmol pimonidazole and 5 µmol BrdU. Four biopsies from SKX, FaDu, and UT-SCC-5 tumors were *ex vivo* exposed to single doses of 0, 2, 4, or 8 Gy (one dose/ biopsy). Due to experimental complications e.g., high necrotic fraction and low numbers of viable cells within a biopsy, using two biopsies per dose per tumor was more applicable for γH2AX foci evaluation. Therefore, two biopsies from Cal33 and UT-SCC-45 tumors received the corresponding dose of the *in vivo* tumor. Immediately after radiation exposure, culture medium was exchanged to remove excess pimonidazole and BrdU. Tumor biopsies were fixed in 4% formalin and embedded in paraffin 24 h post radiation exposure.

Staining, imaging acquisition, and γH2AX evaluation

The immunohistochemical and immunofluorescence staining procedures were previously described [15–17,20]. In brief, two consecutive 3 µm sections of the central part of tumors or biopsies were stained for a) immunohistochemistry (IHC): pimonidazole (Hypoxyprobe, Burlington, MA, USA), BrdU (Agilent Technologies, clone Bu20a, Hamburg, Germany), and counterstained with hematoxylin; or b) immunofluorescence (IF): γH2AX at serine 139 (Merck Millipore, Upstate, clone JBW301, Darmstadt, Germany) and counterstained with 4',6-diamidino-2-phenylindole (DAPI; Invitrogen, Karlsruhe, Germany). ARK™ Kit (Animal Research Kit; Agilent Technologies Deutschland, Hamburg, Germany) and Tyramide Signal Amplification (TSA) Kits #2 (Alexa 488, Life Technologies, Darmstadt, Germany) were applied for IHC and IF, respectively. Image acquisition for IHC and IF was carried out by a fluorescence microscope (Axio Imager M1) equipped with dual cameras (digital color camera: Axiocam MRc, monochrome camera: AxioCam MRm; Carl Zeiss Jena, Jena, Germany) and a

motorized scanning stage (Maerzhaeuser Wetzlar, Wetzlar, Germany). The microscope was controlled by the AxioVison 4.9 software (Carl Zeiss Jena, Jena, Germany). IHC stained sections were scanned with a magnification of 100X using the digital color camera. Subsequently, ten (*in vivo*) regions of interest (ROI) were selected for IF image acquisition. Due to the characteristic of xenograft tumors in which the core of the tumor is highly necrotic, and viable tumor cells are located at the growing outer cell layers, biopsy taken from xenograft tumors contained a low number of analyzable cells located at each end of the biopsy. As a result, five to seven ROIs/ biopsy (*ex vivo*) could be evaluated. The criteria for the ROI selection were as follows; (a) *in vivo*: a single mouse blood vessel surrounded by multiple BrdU positive but pimonidazole negative (oxic) cells; (b) *ex vivo*: tissue at the outer rim of the biopsy with multiple BrdU positive but pimonidazole negative (oxic) cells. For each ROI, a focus stack image (17 individual images with a focus interval of 0.25 μm) at 400X magnification was acquired. All focal planes of the stack image were calculated to a single extended depth of focus image for γH2AX foci evaluation. Within each ROI, oxic cells (*in vivo*: ≤ 45 μm from vessel) with intact nuclei were numbered for randomization and five to ten (*in vivo*) or ten (*ex vivo*) of these nuclei were randomly selected for foci determination. Manual and blinded evaluation of residual γH2AX foci and nuclear area was carried out. Necrotic, apoptotic, S-phase, and differentiated cells were excluded from analysis. Supplement figure 1 shows exemplary images for IHC and IF staining with annotations for foci analysis. Supplement table 1 provides information on total and analyzed numbers of tumors, biopsies and nuclei.

Data processing and statistical analysis

As the nucleus area of the randomly selected nuclei is not homogenously distributed, data were corrected for the nucleus area [15–17,20,25]. Residual corrected foci of an individual nucleus ($cfoci_i$) was calculated by multiplying residual γH2AX foci numbers of an individual nucleus ($foci_i$) with the quotient of the mean nucleus area of the corresponding tumor or biopsy ($\overline{area}$) and the area of the individual nucleus ($area_i$) (Eq. 1).

$$cfoci_i = foci_i \times \left(\frac{\overline{area}}{area_i}\right) \tag{1}$$

Residual normalized foci of an individual nucleus ($nfoci_i$) from an exposed sample were calculated by subtracting $cfoci_i$ from the exposed sample with a mean cfoci of the unexposed tumors or biopsies ($\overline{cfoci_0}$) (Eq. 2). Negative $nfoci_i$ were set to zero under the assumption of no negative irradiation induced foci.

$$nfoci_i = cfoci_i - \overline{cfoci_0} \tag{2}$$

Statistical analysis was performed with SPSS 23 (IBM Deutschland, Ehningen, Germany). Graphs were plotted with GraphPad Prism 7 (GraphPad Software, San Diego, CA, USA).

A mean residual cfoci or nfoci per tumor and biopsy was calculated. The correlation of the mean residual cfoci or nfoci and the radiation doses was determined by linear regression analysis. Analysis of covariance (ANCOVA) was applied to compare the regression slopes and constants (estimated endogenous foci - offsets). The regression slopes and offsets were plotted against previously reported local tumor control data [15,16,21] after single ($TCD_{50(SDambient)}$) or fractionated (30 fractions, 6 weeks; $TCD_{50(30fx/\ 6weeks)}$) radiation exposure under ambient blood flow. The comparability between the procedures was assessed by Bland-Altman analysis. The threshold for statistical significance was defined as $P < 0.05$.

Results

The characteristics of analyzed samples of tumors (*in vivo*) and biopsies (*ex vivo*) were summarized in supplement table 1. Due to predominant necrotic tissue or tumor cell differentiation, analyzable tumors and biopsies ranged between 42.5% (SKX) - 94.4% (Cal33) for the *in vivo* cohort as well as 50.7% (SKX) - 88.9% (Cal33, UT-SCC-45) for the *ex vivo* cohort, respectively. Beside the variations in usable samples, tumor cell density in ROI influenced the total analyzable nuclei ranging *in vivo* from 5,571 (SKX) - 18,790 (Cal33) nuclei and *ex vivo* from 9,851 (SKX) - 37,876 (UT-SCC-5) nuclei. However, equal or lower amounts of analyzable cell nuclei could be found in *ex vivo* biopsies relative to *in vivo* tumors. Supplement figure 1 shows representative images of *in vivo* tumors and *ex vivo* biopsies. The latter showing BrdU positive cells in the outer, oxic tissue rim and a central hypoxic tissue core while *in vivo*, BrdU positive and oxic cells surround the vessels similar to previous reports [15,17,20].

We investigated whether residual γH2AX foci determined in *ex vivo* irradiated biopsies can reflect radiation response of *in vivo* irradiated tumors. Comparison of residual cfoci between tumors and the corresponding biopsies exposed to equivalent doses were analyzed. In all tumor models, a good degree of comparability was observed as indicated by Bland-Altman analysis (Suppl. Fig. 2). A dose dependent linear increase of residual γH2AX cfoci and nfoci was observed in most of tumor models following *in vivo* and *ex vivo* radiation exposure, exempt residual cfoci of *ex vivo* irradiated UT-SCC-5. (cfoci: Suppl Fig 3; Suppl. Table 2; nfoci Fig. 2, Table 1).

The slopes of does response curves (SDRC) of residual nfoci ranged from 0.38 (FaDu) - 1.50 (UT-SCC-45) for *in vivo* irradiated tumors, and from 0.19 (FaDu) - 1.48 (UT-SCC-45) for *ex vivo* irradiated biopsies. With the exemption of FaDu, no statistical difference between the slopes of the *in vivo* and *ex vivo* cohort could be found (Table 1). *Ex vivo* irradiated FaDu biopsies exhibited a significant, ~2-fold lower dose response compared to *in vivo* irradiated tumors (slope of *in vivo*/*ex vivo*; $P < 0.0001$). A similar result was observed in the regression slopes of

residual cfoci except for a significant difference in the offsets of dose response curves (ODRC) between *in vivo* and *ex vivo* cohorts of UT-SCC-45 (Suppl. Table 2).

As previously reported, SDRC of residual nfoci could potentially be used as a radiation response predictor [17]. The SDRC were plotted against the dose needed to control 50% of *in vivo* irradiated tumors locally i.e., TCD$_{50}$, following fractionated (TCD$_{50(30fx/6weeks)}$, Fig. 3A) or single dose irradiation (TCD$_{50(SDambient)}$, Fig. 3B). A range of possible cut-off values for the SDRC (0.55 – 0.7) was determined as it discriminates the tumor models for both TCD$_{50}$ values in a resistant and a sensitive population. Moreover, tumor models with a TCD$_{50(30fx/6weeks)}$ above the clinical standard dose for primary radiotherapy of ~70 Gy showed lower SDRC (≤ 0.55; UT-SCC-5, Cal33, FaDu) while tumor models with lower TCD$_{50(30fx/6weeks)}$ exhibit higher SDRC (≥ 0.7). In contrast, SDRC and ODRC of residual cfoci demonstrated an insufficient potential in the differentiation of radiosensitivity (Suppl. Fig 4).

Discussion

This study is aiming to further enhance the relevance and to translate the γH2AX foci assay as a clinically predictive tool for determining intrinsic radiation sensitivity in tumors. Depending on their intrinsic radiosensitivity, the response to radiation among patients varies considerably [1–7]. Applying a patient-individualized dose based on molecular determinants, omics data, and mathematical modelling could offer an improvement of therapeutic outcomes and an alleviation of normal tissue toxicity [1,4–6,11,14,26,27]. Among molecular-biomarker based assays for the determination of radiation response, the γH2AX foci assay holds a promising potential to become a predictive biomarker in clinical practice [14,16–20,25]. However, it is currently unclear whether γH2AX foci determined in biopsies can reflect and predict the radiation response of the corresponding bulk tumor [14,20,25]. Here, of five hHNSCC models with known radiosensitivity, residual γH2AX foci in irradiated tumors *in vivo* and the corresponding biopsies taken from untreated tumors and irradiated *ex vivo* were evaluated. Radiation response was determined by SDRC of residual γH2AX foci. To assess the predictive value of the assay, the slopes were compared with the previously reported tumor radiosensitivity (TCD$_{50}$) data [15,16,21].

In previous studies, SDRC of residual γH2AX foci demonstrated predictive potential for stratifying experimental tumors and patient-derived tumors based on clinically known intrinsic radiosensitivity tumors [17–19]. However, those studies exclusively assessed radiation induced residual γH2AX foci following *ex vivo* exposure. To our knowledge, this is the first study showing a matching comparison of radiation-induced residual γH2AX foci between locally irradiated tumor xenografts (*in vivo*) and tumor biopsies (*ex vivo*) taken from xenograft tumors prior to radiation exposure. The result demonstrates comparable SDRC of residual

nfoci and cfoci of the *in vivo* irradiated tumors and the *ex vivo* irradiated biopsies in four out of five tumor models. The SDRC values of residual γH2AX nfoci were able to distinguish between radioresistant and radiosensitive models. Generally, a total dose up to 70 Gy is applied in primary radio(chemo)therapy for head and neck cancer (HNC) [28]. Of note, all the evaluated radioresistant tumor models (UT-SCC-5, Cal33, and FaDu) have a fractionated TCD_{50} value higher than the conventional therapeutic dose of 70 Gy. Moreover, the radioresistant tumor models showed that the SDRCs of residual γH2AX nfoci were lower than the proposed cut-off range of 0.55 – 0.7, while the SDRCs of the radiosensitive tumor models (UT-SCC-45 and SKX) were higher than the proposed range. Therefore, a SDRC value might be a suitable indicator for discriminating radiosensitive and radioresistant tumors in the clinics. This is in line with a recent study on HNC patient-derived biopsies reported a similar cut-off of 0.7 for SDRC of residual nfoci [29]. An investigation on additional hHNSCC tumor models and patient-derived materials is ongoing to verify the proposed cut-off range.

The human papillomavirus (HPV) infection status has been shown to be a significant prognostic marker for radiation response of HNSCC. HPV positive HNSCC patients demonstrated a favorable prognosis [30–34] and HPV positive HNC cells are more highly susceptible to radiation compared to HPV negative HNC cells [35,36]. In this study, offsets of dose response curves (ODRC) of residual γH2AX foci did not correlate with the radiation response of the tumor models (Suppl. Fig 4). The HPV negative, and due to a defective DNA damage machinery [23,37], highly radiosensitive model SKX showed a low endogenous γH2AX foci number [16] and low ODRC in the both cohorts. In contrast, the HPV positive UT-SCC-45 model demonstrated an increased radiosensitivity and a high number of endogenous foci [16], which is possibly related to the replication process of HPV. DNA damage proteins including γH2AX, 53BP1 and others are activated and recruited to HPV replication sites to promote viral genome amplification and stability [38,39].

Tumor heterogeneity is among the cellular complexities that greatly encumbers the translation of molecular biomarkers to the clinics [40,41]. In our previous report, a high intratumoral heterogeneity of residual γH2AX foci was detected in hHNSCC models (UT-SCC-5, FaDu, SKX) [20]. Likewise, intratumoral heterogeneity in residual γH2AX foci was more pronounced as compared to intertumoral heterogeneity (data not shown). In line with our previous report, the intra- and intertumoral heterogeneity in the γH2AX foci assay was more pronounced in the *ex vivo* irradiated biopsies than in the *in vivo* irradiated tumors, which probably contributes to the significant difference in the SDRC of residual nfoci and cfoci between the FaDu cohorts [20,25].

Despite the high sensitivity of the γH2AX foci assay, its quantification is labor-intensive and observer-dependent [14]. (Semi-) automated foci counting algorithms [13,42–44] or commercialized software [12,45,46] were implemented in basic- and translational researches. Those algorithms and software are, however, currently unsuitable for tissue specimens due to complex morphological organization of tumor tissues e.g., cells overlap, varying cell types, and complex micromilieu. The evolution of artificial intelligence (AI) has permitted researchers to apply machine learning techniques in microscopy [47], radiology [48], detection of melanomas [49] as well as outcome prediction in colorectal cancer based on recognition of tissue patterns [50]. The advance of AI technology might enable us to overcome the technical challenges in cell and foci recognition process. This could pave the way for the development of a non-biased, reliable automatic foci-counter for solid tissue specimens therewith the assay could potentially be translated, standardized, and implemented as a clinical application in precision radiotherapy [11,14].

In conclusion, with the exception of FaDu tumors, *ex vivo* irradiated biopsies reflected radiation response of *in vivo* irradiated tumors determined by the γH2AX foci assay. Comparable outcomes in γH2AX foci as well as the slopes of dose response curves of residual γH2AX nfoci and cfoci between *in vivo* and *ex vivo* cohorts were observed. Moreover, the SDRC of residual γH2AX nfoci were capable of differentiating radiosensitive and radioresistant tumors based on their intrinsic radioresponsiveness. The outcome of this study needs to be validated in (pre-) clinical studies with a larger cohort. For further classification into more radiation response groups, refinement of the assay by modelling with further biomarkers would be necessary.

Acknowledgements

Competing interest:

institute(s) and for the staff for research funding and collaborations with a multitude of companies worldwide.

For the German Cancer Research Center (DKFZ, Heidelberg) Dr. Baumann is on the supervisory boards of HI-STEM gGmbH (Heidelberg).

For the present study, Dr. Baumann confirms that none of the above mentioned funding sources were involved in the study design or materials used, nor in the collection, analysis and interpretation of data nor in the writing of the paper.

Treewut Rassamegevanon, Steffen Löck, Mechthild Krause, and Cläre von Neubeck declare no competing interests.

References

[1] Caudell JJ, Torres-Roca JF, Gillies RJ, Enderling H, Kim S, Rishi A, et al. The future of personalised radiotherapy for head and neck cancer. Lancet Oncol 2017;18:e266–73. doi:10.1016/S1470-2045(17)30252-8.

[2] Forker LJ, Choudhury A, Kiltie AE. Biomarkers of Tumour Radiosensitivity and Predicting Benefit from Radiotherapy. Clin Oncol 2015;27:561–9. doi:10.1016/j.clon.2015.06.002.

[3] West CM, Davidson SE, Roberts SA, Hunter RD. The independence of intrinsic radiosensitivity as a prognostic factor for patient response to radiotherapy of carcinoma of the cervix. Br J Cancer 1997;76:1184–90.

[4] Scott JG, Berglund A, Schell MJ, Mihaylov I, Fulp WJ, Yue B, et al. A genome-based model for adjusting radiotherapy dose (GARD): a retrospective, cohort-based study. Lancet Oncol 2017;18:202–11. doi:10.1016/S1470-2045(16)30648-9.

[5] Bibault J-E, Fumagalli I, Ferté C, Chargari C, Soria J-C, Deutsch E. Personalized radiation therapy and biomarker-driven treatment strategies: a systematic review. Cancer Metastasis Rev 2013;32:479–92. doi:10.1007/s10555-013-9419-7.

[6] Baumann M, Krause M, Overgaard J, Debus J, Bentzen SM, Daartz J, et al. Radiation oncology in the era of precision medicine. Nat Rev Cancer 2016;16:234–49. doi:10.1038/nrc.2016.18.

[7] Yaromina A, Krause M, Baumann M. Individualization of cancer treatment from radiotherapy perspective. Mol Oncol 2012;6:211–21. doi:10.1016/j.molonc.2012.01.007.

[8] Rogakou EP, Pilch DR, Orr AH, Ivanova VS, Bonner WM. DNA double-stranded breaks induce histone H2AX phosphorylation on serine 139. J Biol Chem 1998;273:5858–68. doi:10.1074/JBC.273.10.5858.

[9] Taneja N, Davis M, Choy JS, Beckett MA, Singh R, Kron SJ, et al. Histone H2AX phosphorylation as a predictor of radiosensitivity and target for radiotherapy. J Biol Chem 2004;279:2273–80. doi:10.1074/jbc.M310030200.

[10] Ivashkevich AN, Martin OA, Smith AJ, Redon CE, Bonner WM, Martin RF, et al. γH2AX foci as a measure of DNA damage: a computational approach to automatic analysis. Mutat Res 2011;711:49–60. doi:10.1016/j.mrfmmm.2010.12.015.

[11] Reddig A, Rübe CE, Rödiger S, Schierack P, Reinhold D, Roggenbuck D. DNA damage assessment and potential applications in laboratory diagnostics and precision medicine. J Lab Precis Med 2018;3:31–31. doi:10.21037/jlpm.2018.03.06.

[12] Rothkamm K, Barnard S, Ainsbury EA, Al-hafidh J, Barquinero J-F, Lindholm C, et al. Manual versus automated γ-H2AX foci analysis across five European laboratories: Can this assay be used for rapid biodosimetry in a large scale radiation accident? Mutat Res Toxicol Environ Mutagen 2013;756:170–3. doi:10.1016/j.mrgentox.2013.04.012.

[13] Pilch DR, Sedelnikova OA, Redon C, Celeste A, Nussenzweig A, Bonner WM. Characteristics of γ-H2AX foci at DNA double-strand breaks sites. Biochem Cell Biol 2003;81:123–9. doi:10.1139/o03-042.

[14] Willers H, Gheorghiu L, Liu Q, Efstathiou JA, Wirth LJ, Krause M, et al. DNA Damage Response Assessments in Human Tumor Samples Provide Functional Biomarkers of Radiosensitivity. Semin Radiat Oncol 2015;25:237–50. doi:10.1016/J.SEMRADONC.2015.05.007.

[15] Menegakis A, Eicheler W, Yaromina A, Thames HD, Krause M, Baumann M. Residual DNA double strand breaks in perfused but not in unperfused areas determine different radiosensitivity of tumours. Radiother Oncol 2011;100:137–44. doi:10.1016/J.RADONC.2011.07.001.

[16] Koch U, Höhne K, von Neubeck C, Thames HD, Yaromina A, Dahm-Daphi J, et al. Residual γH2AX foci predict local tumour control after radiotherapy. Radiother Oncol 2013;108:434–9. doi:10.1016/J.RADONC.2013.06.022.

[17] Menegakis A, von Neubeck C, Yaromina A, Thames H, Hering S, Hennenlotter J, et al. γH2AX assay in ex vivo irradiated tumour specimens: A novel method to determine tumour radiation sensitivity in patient-derived material. Radiother Oncol 2015;116:473–9. doi:10.1016/J.RADONC.2015.03.026.

[18] De-Colle C, Yaromina A, Hennenlotter J, Thames H, Mueller AC, Neumann T, et al. Ex vivo γH2AX radiation sensitivity assay in prostate cancer: Inter-patient and intra-patient heterogeneity. Radiother Oncol 2017;124:386–94. doi:10.1016/j.radonc.2017.08.020.

[19] Menegakis A, De Colle C, Yaromina A, Hennenlotter J, Stenzl A, Scharpf M, et al. Residual γH2AX foci after ex vivo irradiation of patient samples with known tumour-type specific differences in radio-responsiveness. Radiother Oncol 2015;116:480–5. doi:10.1016/J.RADONC.2015.08.006.

[20] Rassamegevanon T, Löck S, Range U, Krause M, Baumann M, von Neubeck C. Tumor heterogeneity determined with a γH2AX foci assay: A study in human head and neck

squamous cell carcinoma (hHNSCC) models. Radiother Oncol 2017;124:379–85. doi:10.1016/J.RADONC.2017.06.027.

[21] Yaromina A, Thames H, Zhou X, Hering S, Eicheler W, Dörfler A, et al. Radiobiological hypoxia, histological parameters of tumour microenvironment and local tumour control after fractionated irradiation. Radiother Oncol 2010;96:116–22. doi:10.1016/J.RADONC.2010.04.020.

[22] Yaromina A, Krause M, Thames H, Rosner A, Krause M, Hessel F, et al. Pre-treatment number of clonogenic cells and their radiosensitivity are major determinants of local tumour control after fractionated irradiation. Radiother Oncol 2007;83:304–10. doi:10.1016/J.RADONC.2007.04.020.

[23] Kasten-Pisula U, Menegakis A, Brammer I, Borgmann K, Mansour WY, Degenhardt S, et al. The extreme radiosensitivity of the squamous cell carcinoma SKX is due to a defect in double-strand break repair. Radiother Oncol 2009;90:257–64. doi:10.1016/J.RADONC.2008.10.019.

[24] Koi L, Löck S, Linge A, Thurow C, Hering S, Baumann M, et al. EGFR-amplification plus gene expression profiling predicts response to combined radiotherapy with EGFR-inhibition: A preclinical trial in 10 HNSCC-tumour-xenograft models. Radiother Oncol 2017;124:496–503. doi:10.1016/J.RADONC.2017.07.009.

[25] Rassamegevanon T, Löck S, Baumann M, Krause M, Neubeck C von. Heterogeneity of γH2AX foci increases in ex vivo biopsies relative to in vivo tumors. Int J Mol Sci 2018;19:2616. doi:10.3390/ijms19092616.

[26] McMahon SJ, Schuemann J, Paganetti H, Prise KM. Mechanistic Modelling of DNA Repair and Cellular Survival Following Radiation-Induced DNA Damage. Sci Rep 2016;6:33290. doi:10.1038/srep33290.

[27] Knijnenburg TA, Wang L, Zimmermann MT, Chambwe N, Gao GF, Cherniack AD, et al. Genomic and Molecular Landscape of DNA Damage Repair Deficiency across The Cancer Genome Atlas. Cell Rep 2018;23:239–254.e6. doi:10.1016/j.celrep.2018.03.076.

[28] Colevas AD, Yom SS, Pfister DG, Spencer S, Adelstein D, Adkins D, et al. NCCN Guidelines Insights: Head and Neck Cancers, Version 1.2018. J Natl Compr Cancer Netw 2018;16:479–90. doi:10.6004/JNCCN.2018.0026.

[29] Meneceur S, Löck S, Gudziol V, Hering S, Bütof R, Rehm M, et al. Residual gammaH2AX foci in head and neck squamous cell carcinomas as predictors for tumour radiosensitivity : Evaluation in pre-clinical xenograft models and clinical specimens. Radiother Oncol 2019;137:24–31. doi:10.1016/j.radonc.2019.04.009.

[30] Vokes EE, Agrawal N, Seiwert TY. HPV-Associated Head and Neck Cancer. J Natl Cancer Inst 2015;107:djv344. doi:10.1093/jnci/djv344.

[31] Linge A, Schötz U, Löck S, Lohaus F, von Neubeck C, Gudziol V, et al. Comparison of detection methods for HPV status as a prognostic marker for loco-regional control after radiochemotherapy in patients with HNSCC. Radiother Oncol 2018;127:27–35. doi:10.1016/J.RADONC.2017.12.007.

[32] Linge A, Lohaus F, Löck S, Nowak A, Gudziol V, Valentini C, et al. HPV status, cancer stem cell marker expression, hypoxia gene signatures and tumour volume identify good prognosis subgroups in patients with HNSCC after primary radiochemotherapy: A multicentre retrospective study of the German Cancer Consortium Radiation Oncology Group (DKTK-ROG). Radiother Oncol 2016;121:364–73. doi:10.1016/J.RADONC.2016.11.008.

[33] Adelstein D, Gillison ML, Pfister DG, Spencer S, Adkins D, Brizel DM, et al. NCCN Guidelines Insights: Head and Neck Cancers, Version 2.2017. J Natl Compr Canc Netw 2017;15:761–70. doi:10.6004/jnccn.2017.0101.

[34] Lohaus F, Linge A, Tinhofer I, Budach V, Gkika E, Stuschke M, et al. HPV16 DNA status is a strong prognosticator of loco-regional control after postoperative radiochemotherapy of locally advanced oropharyngeal carcinoma: Results from a multicentre explorative study of the German Cancer Consortium Radiation Oncology Group (DKTK-ROG). Radiother Oncol 2014;113:317–23. doi:10.1016/J.RADONC.2014.11.011.

[35] Kimple RJ, Smith MA, Blitzer GC, Torres AD, Martin JA, Yang RZ, et al. Enhanced radiation sensitivity in HPV-positive head and neck cancer. Cancer Res 2013;73:4791–800. doi:10.1158/0008-5472.CAN-13-0587.

[36] Rieckmann T, Tribius S, Grob TJ, Meyer F, Busch CJ, Petersen C, et al. HNSCC cell lines positive for HPV and p16 possess higher cellular radiosensitivity due to an impaired DSB repair capacity. Radiother Oncol 2013;107:242–6. doi:10.1016/j.radonc.2013.03.013.

[37] Mansour WY, Bogdanova N V., Kasten-Pisula U, Rieckmann T, Köcher S, Borgmann K, et al. Aberrant overexpression of miR-421 downregulates ATM and leads to a pronounced DSB repair defect and clinical hypersensitivity in SKX squamous cell carcinoma. Radiother Oncol 2013;106:147–54. doi:10.1016/J.RADONC.2012.10.020.

[38] Spence T, Bruce J, Yip KW, Liu F-F. HPV Associated Head and Neck Cancer. Cancers (Basel) 2016;8. doi:10.3390/cancers8080075.

[39] Gautam D, Moody CA. Impact of the DNA Damage Response on Human Papillomavirus Chromatin. PLOS Pathog 2016;12:e1005613. doi:10.1371/journal.ppat.1005613.

[40] Cyll K, Ersvær E, Vlatkovic L, Pradhan M, Kildal W, Avranden Kjær M, et al. Tumour heterogeneity poses a significant challenge to cancer biomarker research. Br J Cancer 2017;117:367–75. doi:10.1038/bjc.2017.171.

[41] Hanahan D, Weinberg RA. Hallmarks of cancer: the next generation. Cell 2011;144:646–74. doi:10.1016/j.cell.2011.02.013.

[42] Feng J, Lin J, Zhang P, Yang S, Sa Y, Feng Y. A novel automatic quantification method for high-content screening analysis of DNA double strand-break response. Sci Rep 2017;7:9581. doi:10.1038/s41598-017-10063-0.

[43] Lapytsko A, Kollarovic G, Ivanova L, Studencka M, Schaber J. FoCo: a simple and robust quantification algorithm of nuclear foci. BMC Bioinformatics 2015;16:392. doi:10.1186/s12859-015-0816-5.

[44] Oeck S, Malewicz NM, Hurst S, Rudner J, Jendrossek V. The Focinator - a new open-source tool for high-throughput foci evaluation of DNA damage. Radiat Oncol 2015;10:163. doi:10.1186/s13014-015-0453-1.

[45] Willitzki A, Lorenz S, Hiemann R, Guttek K, Goihl A, Hartig R, et al. Fully automated analysis of chemically induced γH2AX foci in human peripheral blood mononuclear cells by indirect immunofluorescence. Cytom Part A 2013;83:1017–26. doi:10.1002/cyto.a.22350.

[46] Sowa M, Reddig A, Schierack P, Reinhold D, Roggenbuck D. Phosphorylated histone 2AX foci determination in capillary blood mononuclear cells. J Lab Precis Med 2018;3:45–45. doi:10.21037/jlpm.2018.04.02.

[47] Rivenson Y, Göröcs Z, Günaydin H, Zhang Y, Wang H, Ozcan A. Deep learning microscopy. Optica 2017;4:1437. doi:10.1364/OPTICA.4.001437.

[48] Hosny A, Parmar C, Quackenbush J, Schwartz LH, Aerts HJWL. Artificial intelligence in radiology. Nat Rev Cancer 2018;18:500–10. doi:10.1038/s41568-018-0016-5.

[49] Haenssle HA, Fink C, Schneiderbauer R, Toberer F, Buhl T, Blum A, et al. Man against machine: diagnostic performance of a deep learning convolutional neural network for dermoscopic melanoma recognition in comparison to 58 dermatologists. Ann Oncol 2018;29:1836–42. doi:10.1093/annonc/mdy166.

[50] Bychkov D, Linder N, Turkki R, Nordling S, Kovanen PE, Verrill C, et al. Deep learning based tissue analysis predicts outcome in colorectal cancer. Sci Rep 2018;8:3395. doi:10.1038/s41598-018-21758-3.
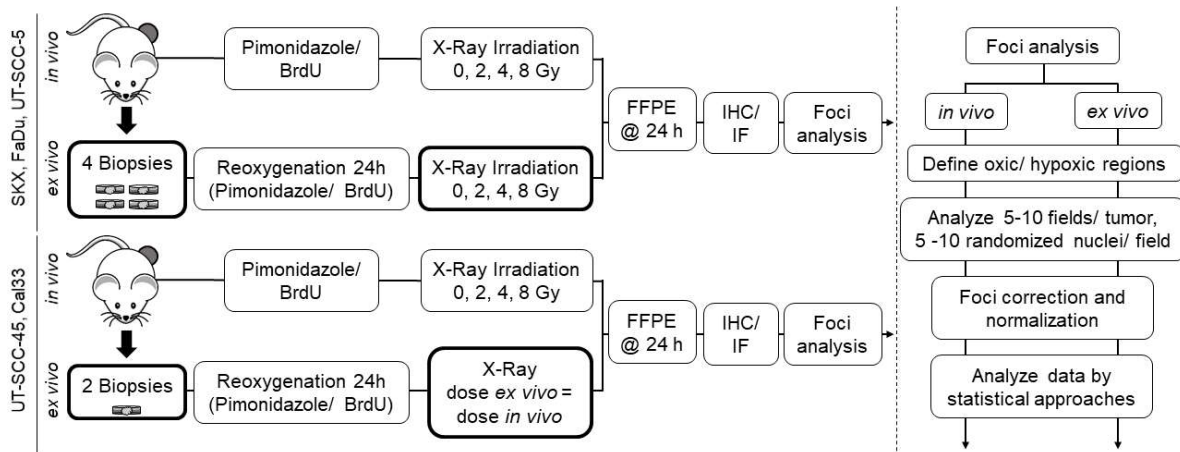
Fig. 1. Overview of the experimental workflow and γH2AX foci analysis procedures

In vivo: after recovery from anesthesia, mice were injected with pimonidazole and BrdU 1 h prior to a single dose radiation exposure with 0, 2, 4, or 8 Gy. *Ex vivo*: Four biopsies from anesthetized mice bearing SKX, FaDu, and UT-SCC-5 tumors were taken and each biopsy was *ex vivo* exposed to a single dose irradiation of 0, 2, 4, or 8 Gy (one biopsy/ dose). Due to experimental complications e.g., high necrotic fraction and low numbers of viable cells within a biopsy, the experimental protocol was adapted for Cal33 and UT-SCC-45. Here two biopsies per tumors were taken and exposed to a single dose irradiation corresponding to the dose applied for the *in vivo* tumor. Tumors and biopsies were fixed in formalin and embedded in paraffin. Gamma H2AX foci were enumerated and analyzed. (IHC: Immunohistochemistry, IF: Immunofluorescence, FFPE: Formalin-Fixed Paraffin-Embedded)
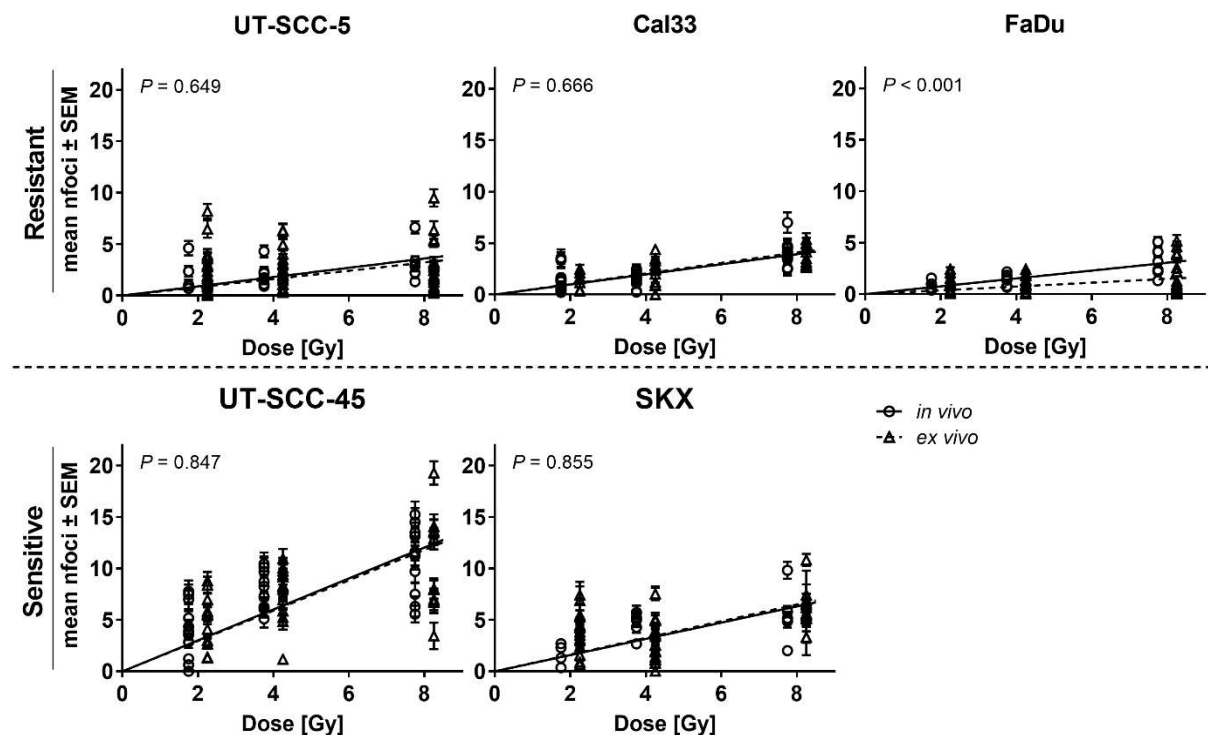

Fig. 2. Dose response curves of residual γH2AX nfoci of *in vivo* irradiated tumors and *ex vivo* irradiated biopsies.

Linear regression analysis of residual γH2AX nfoci (24 h post irradiation) as a function of radiation dose was performed across five hHNSCC tumor models. Symbols (open circle: *in vivo*; open triangle: *ex vivo*) and error bars represent mean nfoci and standard error of mean

(SEM), respectively. The regression constant was adjusted to zero. ANCOVA was applied to compare between the slopes of the dose response curves of irradiated tumors and irradiated biopsies for each tumor model (Table 1).
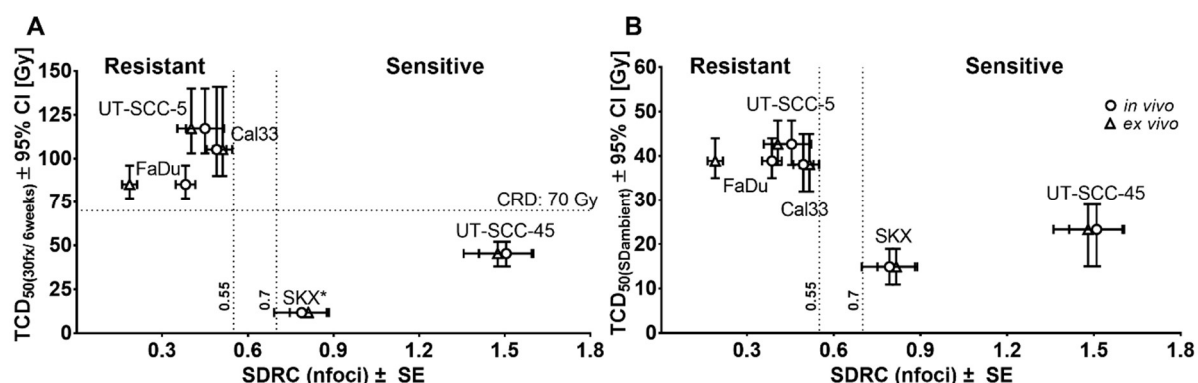

Fig. 3. Classification of radiation sensitivity based on tumor control dose 50% (TCD$_{50}$) and slope of dose response curve (SDRC) of residual γH2AX nfoci

TCD$_{50(30fx/6weeks)}$ (A) or TCD$_{50(SDambient)}$ (B) and slopes of the residual γH2AX nfoci dose response curves of the *in vivo* (open circle) and *ex vivo* (open triangle) cohort were plotted. The TCD$_{50}$ values were previously published [15,16,21]. Error bars represent 95% confidence intervals (95% CI) and standard errors (SE) for TCD$_{50}$ values and the SDRC, respectively. The vertical dotted lines at SDRC = 0.55 and 0.7 represent a possible range of the SDRC for the classification between resistant and sensitive tumors. The horizontal dotted line represents the conventional clinical radiation dose (CRD = 70 Gy) for head and neck cancer treatment. Note: Different scaling on y-axis, TCD$_{50(12fx/6weeks)}$ was used for SKX due to its high radiosensitivity.

Table 1. Linear regression analysis of residual γH2AX nfoci dose response of *in vivo* irradiated tumors and *ex vivo* irradiated biopsies from five hHNSCC models. The differences of the slopes of the dose response curves (SDRC) between the *in vivo* irradiated tumors and the *ex vivo* irradiated biopsies for each tumor model were determined by ANCOVA. TCD$_{50}$ after irradiation with single dose under ambient condition (SD$_{ambient}$) and 30 fractions within 6 weeks (30fx/ 6 weeks) are shown.

		Resistant			Sensitive	
		UT-SCC-5	Cal33	FaDu	UT-SCC-45	SKX
in vivo	Slope [± SE]	0.45 ± 0.07	0.49 ± 0.04	0.38 ± 0.03	1.5 ± 0.10	0.79 ± 0.10
	95% CI	0.31; 0.59	0.42; 0.56	0.31; 0.45	1.31; 1.70	0.58; 1.00
	P value	<0.0001	<0.0001	<0.0001	<0.0001	<0.0001
ex vivo	Slope [± SE]	0.40 ± 0.05	0.51 ± 0.03	0.19 ± 0.03	1.48 ± 0.12	0.81 ± 0.06
	95% CI	0.31; 0.50	0.44; 0.58	0.13; 0.24	1.23; 1.72	0.68; 0.94
	P value	<0.0001	<0.0001	<0.0001	<0.0001	<0.0001
P value (Significance between slopes)		0.649	0.666	**<0.001**	0.847	0.855
TCD$_{50 (30fx/ 6 weeks)}$[16,21] [95%CI]		117.2 [103; 140]	105.2 [90; 141]	85.2 [77; 96]	45.4 [38; 52]	11.76 [11.3; 12.2][a,b]
TCD$_{50 (SDambient)}$[15,21] [95%CI]		42.7 [38; 48]	38.1 [32; 45]	38.9 [35; 44]	23.3 [15; 29]	14.9 [10.9; 18.9]

[a] Standard deviation

b TCD$_{50}$ fx values after irradiation with 12 fractions within 6 weeks